The early events after the June 17 2000 mainshock in South Iceland: constraints for instantaneous dynamic triggering with rate- and state-dependent friction

M. E. Belardinelli [1], A. Antonioli [2], A. Bizzarri [3], K.S. Vogfjord [4]

[1] Department of Physics, University of Bologna, Italy (elina@ibogfs.df.unibo.it); [2] Istituto Nazionale di Geofisica e Vulcanologia, Rome, Italy (antonioli@ingv.it); [3] Istituto Nazionale di Geofisica e Vulcanologia, Bologna, Italy (bizzarri@bo.ingv.it); [4] Icelandic Meteorological Office, Physics Department, Reykjavik, Iceland (vogfjord@vedur.is)

ABSTRACT.

We analyze the coseismic stress redistribution during the seismic sequence of June 17, 2000 in South Iceland in which a mainshock (M_S 6.6) was followed by three quite large events within few tens of seconds (8, 26 and 30 s respectively) at a distance up to about 90 km. We use this observational case to investigate the possibility of fault interaction by purely transient coseismic stress changes and in particular nearly instantaneous triggering. We compute the stress changes as functions of time in a stratified elastic half space by means of the discrete wavenumber and reflectivity method (Cotton and Coutant, 1997). We evaluate the dynamic stresses caused by the mainshock at the hypocenter of the three subsequent events. Our results show that the onset of the last two events is slightly delayed with respect to the arrival time of the second positive peak of Coulomb Failure Function variation, while the first event stroked after the first positive peak. We also analysed the response of a rate- and state-dependent spring-slider model of fault perturbed by the shear stress and the normal stress variations that we computed as generated by the June 17, 2000 mainshock at the three hypocenters. Assuming an initial sliding velocity comparable with tectonic velocity of the region, for the last two events, we obtained failure times close to the observed origin times, provided that the value of the initial effective normal stress is low enough, whereas the 8 s event requires closer to failure initial conditions to be reproduced. The 8 s event might already be close to failure at the time of the mainshock, due to its vicinity to the main event and the subsequent June 21 (MS 6.6) mainshock. Therefore the first aftershock does not provide us a clear evidence of dynamic triggering.

1. The June 2000 seismic sequence in South Iceland

The South Iceland Seismic Zone (SISZ in Fig. 1) is a left lateral E-W transform zone that connects the Western Volcanic Zone (WVZ) and the Reykjanes Peninsula (RP) oblique rift zone in the west to the Eastern Volcanic Zone (EVZ) in the east.

On June 17 2000, a seismic sequence started in the SISZ and the Reykjanes Peninsula (RP in Fig. 1) with an event of magnitude M_S=6.6 at 14:40:41 UTC. The hypocenter location was 63.973°N, 20.367°W and 6.3 km depth. A second large event (M_S=6.6) occurred on June 21, at about 17 km west of the June 17 event, at 63.972°N, 20.711°W and 5.0 km depth.

The sequence was very well monitored by several local networks: digital seismic stations, strong motion network, volumetric strain meter networks and permanent GPS stations in Iceland. Coseismic deformations were measured by GPS stations and InSAR measurements allowing to estimate the distributed slip models of the two major events (Pedersen et al., 2003).

Three early events were detected in the first minute after the June 17 earthquake (Vogfjord, 2003). Two events occurred **26** s and **30** s after the mainshock, at a distance of 65 km and 77 km, respectively, and with an estimated magnitude M_w=5.5. Another event with a smaller magnitude (M_l= 3.5), occurred **8** s after the June 17 at 25 km distance (Table 1 and Fig. 1). The origin time of these events correlates with the arrival time of seismic waves generated by the June 17 mainshock, as they swept westward, suggesting a causative link between them and the mainshock of June 17 2000 in the SISZ. We investigate this possibility by analyzing the temporal evolution of the stress generated by the mainshock at the hypocenters of these three early events.

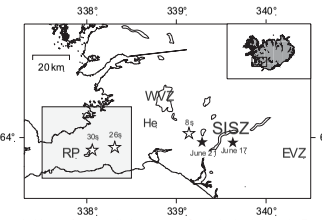

Figure 1. Map of the studied area: the South Iceland Seismic Zone (SISZ) and the Reykjanes Peninsula (RP). The epicenter locations of the two largest events of the June 2000 sequence (June 17 and June 21) are shown by the dark stars and the three largest aftershocks of the June 17 mainshock are shown by white stars, with their origin times (s) relative to the mainshock. The shaded area delimites the map shown in figure 3. The inset map of Iceland shows the study area. "He" marks the location of Hengill volcano."WVZ" and "EVZ" indicate the West Volcanic Zone and East Volcanic Zone, respectively.

Table 1. Aftershock parameters (SIl network)

Origin time (hh mm ss)	Latitude (°)	Longitude (°)	Depth (km)	M_l
15:40:49	64.020	-20.86	9.0	~3.5
15:41:07	63.951	-21.69	8.9	~5.5
15:41:11	63.937	-21.94	3.8	~5.5

2. Dynamic stress interaction

Both the 26 s and 30 s events occurred in a region of negligible static stress changes caused by the mainshock of June 17 2000 (Arnadottir et al., 2003). Therefore fault interaction due to static stress changes can be discarded to interpret them. We use these observational cases to investigate the possibility of fault interaction by purely transient coseismic stress changes.

We compute the stress field variations as a function of time, $\Delta\sigma_{ij}(t)$, due to the June 17 2000 mainshock, using the discrete wave-number and reflectivity code developed by Cotton and Coutant (1997). We assumed a four layer structure inferred from tomographic studies for the East of Hengill region ('He' in Fig. 1), where the June 17 mainshock and the 8 s event are located, since the largest part of the wave path from the mainshock to the aftershocks in the RP (26 s and 30 s events) is East of Hengill.

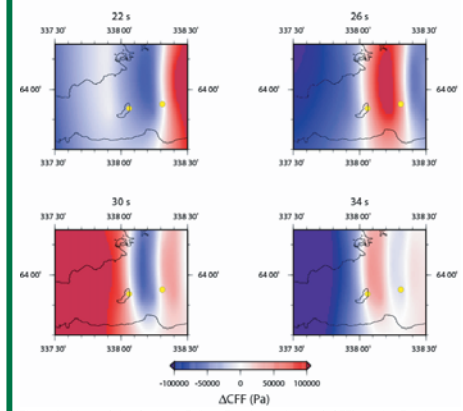

Figure 2. Maps of the Coulomb Failure Function variations (ΔCFF) on the Reykjanes Peninsula (RP) region. The yellow dots are the epicentral locations of the two M_L>5 dynamically triggered aftershocks (at 26 s and 30 s after the mainshock). The maps are computed at a depth of 8.9 km (the 26 s event depth, Table 1). The black solid curve is the coastal line of the RP. Snap shots are shown for 22, 26, 30 and 34 seconds.

For the main event (June 17), we assume a bilateral rupture in a Haskell source model with rise times variable in the range 1-2 s and 2.5 km/s rupture velocity. The slip distribution on the fault plane is that shown by Arnadottir et al. (2003), as retrieved by a joint inversion of GPS and InSAR data . The fault parameters for the mainshock lay within a narrow range of estimated values; we adopted a strike angle of 7°, a dip of 86° and a rake of 180° (right lateral strike slip mechanism), on the basis of the aftershocks distribution.

The Coulomb Failure Function variation is evaluated as follows

$$\Delta CFF(t) = \Delta\tau(t) + \mu_s \Delta\sigma(t)$$

where μ_s is the apparent friction coefficient ($\mu_s=(1-\beta)\mu$ with μ friction coefficient and β Skempton coefficient); $\Delta\tau(t)$ and $\Delta\sigma(t)$ are the shear stress change and the normal stress change (the latter assumed positive for extension in this section) on right lateral N-S vertical fault planes (in agreement with the averaged features of the identified structures of the area). All times are evaluated so that the mainshock origin time is *t=0*.

Either horizontal maps of ΔCFF evolution in the Reykjanes Peninsula (Fig. 2) and the stress evolution evaluated in the hypocenter of the three early events (Fig. 3) show that the arrival times of positive peaks of stress waves are slightly advanced with respect to the aftershock origin times.

For the 8 s event (Fig. 3a), the negative normal stress counteracts the effect of the shear stress. As a result, the ΔCFF dynamic peaks are lower than corresponding peaks in $\Delta\tau$. The timing of the rupture is delayed about two seconds with respect to the first peak of ΔCFF at $t=t'$.

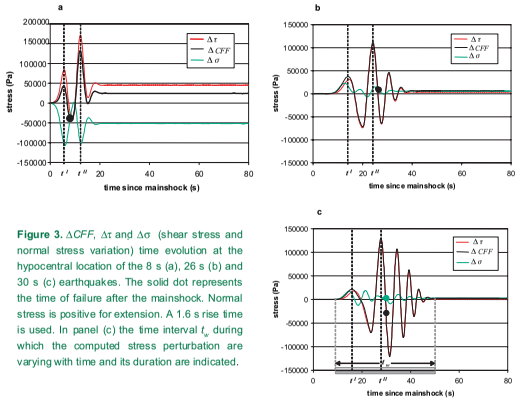

Figure 3. ΔCFF, $\Delta\tau$ and $\Delta\sigma$ (shear stress and normal stress variation) time evolution at the hypocentral location of the 8 s (a), 26 s (b) and 30 s (c) earthquakes. The solid dot represents the time of failure after the mainshock. Normal stress is positive for extension. A 1.6 s rise time is used. In panel (c) the time interval t_w during which the computed stress perturbation are varying with time and its duration are indicated.

In the hypocenter of the other two events (Fig. 3b,c), $\Delta\sigma$ is negligible with respect to $\Delta\tau$ and the static values, reached after about 50 s, are negligible with respect to the dynamic peaks, as expected. Both the 26 s and the 30 s events did not occur immediately at the first arrival time of the seismic waves generated by the main event, but they followed closely (about two seconds) the second peak of ΔCFF at t'', whose amplitude is more than twice the first positive peak. These results could support the idea of dynamic triggering as a possible explanation of the aftershocks on the Reykjanes peninsula.

3. Instantaneous triggering: a test with a spring-slider model

Observations suggest that the three early events followed closely the arrival of seismic waves at their location, or, at least, they occurred within the time interval during which the dynamic seismic signal was above the background noise level. In the previous section we found that the origin times of the three aftershocks followed the arrival time of positive peaks of ΔCFF at their hypocenters, being about two seconds later. The three early events could represent evidences of **instantaneous triggering**, a particular case of fault interaction that occurs within the time interval t_w (fig. 4c) during which the transient stress signal generated by an earthquake is not vanishing in the location of another fault (where a second earthquake can be triggered).

To verify the feasibility of this effect in terms of the rheology of the triggered fault we performed several tests by means of a spring-slider model of fault. We applied to this system the stress perturbations $\Delta\tau(t)$ and $\Delta\sigma(t)$ evaluated for the three early events, as explained in the previous section and we studied the spring-slider parameters suitable to have perturbed failure times t_p (when the sliding velocity of the perturbed fault exceeds V_*=10 cm/s) that are close to the origin time of each event, as in the case shown in Figure 4.

We assume a rate- and state-dependent friction τ_f, (Linker and Dieterich, 1992) for an applied time-dependent normal stress σ (in this section assumed positive for compression) with $\sigma=\sigma_0+\Delta\sigma(t)$, σ_0 effective normal stress before the perturbed earthquake. Indicating with $V=d\delta/dt$ and Ψ the sliding velocity and the state variable at a time t, respectively, the spring-slider fault is described by the following set of equations

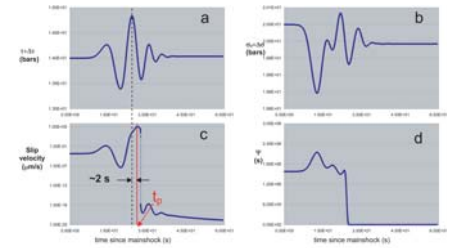

Figure 4. Dynamic instantaneous response of a spring-slider system to the stress perturbation $\Delta\tau(t)$ and $\Delta\sigma(t)$ obtained in the 26 s aftershock hypocenter with a 2 s rise time for the June 17 mainshock. In panel (a) we represent the evolution of the total loading traction, in panel (b) the total effective normal stress (positive for compression). In panel (c) the sliding velocity is shown as a function of time with indication of the failure instant of time t_p when the sliding velocity exceeds V_*=10 cm/s. In panel (d) the state variable evolution is represented. We assumed parameters values as in Table 2 and in the text, with α=0.3. The ~2 s triggering delay of the fault response with respect to the time instant of the second peak of applied shear stress is indicated.

$$\tau_f(V,\Psi,t) = \left[\mu_* + a\ln\left(\frac{V}{V_*}\right) + b\ln\left(\frac{\Psi V_*}{L}\right)\right]\sigma(t)$$

$$\dot{\Psi} = 1 - \frac{\Psi V}{L} - \alpha\frac{\Psi\dot{\sigma}}{b\sigma}$$

$$m\dot{V} = \tau + \Delta\tau(t) - \tau_f$$

where m is the mass per unit surface and $\tau=k(\delta_0-\delta)$, with δ_0 loading point displacement.

We consider values of the parameter α that controls the sensitivity of friction to normal stress changes in the experimental range 0.25-0.5. If $\alpha=0$, only the shear traction perturbation $\Delta\tau(t)$ is applied. The reference values of model parameters are listed in Table 2, unless differently specified. We use a value of $V_*=V_0=d\delta_0/dt$=2 cm/yr, equal to the spreading rate in the SISZ. The initial conditions of the fault are $V_i=V(t=0)=V_0$ and $\Psi(t=0)=L/V_i$: the fault is then assumed to be at steady state at the loading point velocity. For the chosen initial conditions and parameters values, we find that t_p, the first instant of failure in unperturbed conditions ($\Delta\tau(t)=\Delta\sigma(t)=0$), is around tens of years with varying the effective normal prestress value σ_0 between 20 and 1000 bars.

We obtain a "short term" response of the fault (indicating instantaneous dynamic triggering) only for small values of the effective normal stress (less than 40 bars), as summarized in Table 3 for 1.6 s mainshock rise time .
The differences between our estimates of the failure time of the three early events and their origin time in Table 3 might be reduced assuming a more complex model of fault response.

Table 2. Fault failure parameters

μ_*	0.7
a	$3\ 10^{-3}$
b	10^{-2}
L (μm)	10^3
α	0.3
m (kg/m²)	$1.9\ 10^6$
k (bar/μm)	3.10^{-5}
V_i (cm/yr)	2
V_0 (cm/yr)	2
V_* (m/s)	0.1

Table 3. Summary of results for a 1.6 s mainshock rise time.

Origin time (s)	7.8+/-0.1	25.9+/-0.1	30.3 +/-0.2
t' (s)	5.86	14.06	16.41
$\Delta CFF(t')$ (MPa)	0.043	0.037	0.021
t'' (s)	12.2	24.14	27.89
$\Delta CFF(t'')$ (MPa)	0.132	0.111	0.129
t_p (s)	12.5-13.5	24.6-24.9	28.0-29.1
σ_0 (bar)	15-30	15-20	15-30

With larger values of the effective normal stress than in Table 3 we obtain a "long term" or delayed response of the fault, where the failure time t_p is generally well after the end of the time varying part of the stress perturbation (Fig. 5). The parameter α was found to affects the fault response mainly in the long term, as depending on the particular stress perturbation history applied (the effect on the 8 s aftershock differs from the 26 s aftershock, Fig. 5 a,b).

In the case of the 8 s aftershock, the short term response for low values σ_0 does not provide a t_p value enough closed to 8 s (Table 3). We reproduced the origin time of the first event using closer to failure initial conditions than previously specified (V_i=20 m/yr and $\Psi(t=0)=1.2\ L/V_i$). For these reasons the 8 s event does not provide us fully convincing evidence of dynamic triggering due to the June 17, 2000 mainshock and we are inclined to interpret the 8 s source fault as already going to fail at the time of the mainshock. To support this we may observe that the 8 s event is in the near field of the June 17, 2000 mainshock and in the very near field of the subsequent mainshock of June 21 2000 in the SISZ (Fig. 1).

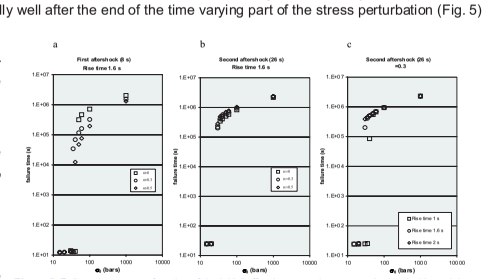

Figure 5. Failure time t_p as a function of the initial effective normal stress σ_0 obtained with applying the stress history $\Delta\tau(t)$ and $\Delta\sigma(t)$ computed in the 8 s hypocenter (panel (a)), in the 26 s aftershock hypocenter (panel (b)), and for three values of the α parameter. A 1.6 s rise time for the june 17 mainshock is assumed. In panel (c) we consider α=0.3 and different stress perturbations $\Delta\tau(t)$ and $\Delta\sigma(t)$ evaluated at the 26 s hypocenter with varying the rise time of the June 17 mainshock. Parameter values are those reported in Table 2 and in the text. A short term response of the fault (t_p ~tens of seconds) is evident only for low values of effective normal prestress ($\sigma_0 \leq$ 35 bars). In these cases t_p tends to follow a peak of the applied shear stress perturbation, $\Delta\tau(t)$, by 2 s or less.

With varying the rise time of the mainshock, the a parameter and the initial conditions, in order to have instantaneous triggering for all the events we found a threshold ρ_{min} in the ratio $\rho=\Delta\tau/\partial\sigma_0$, where $\Delta\tau$ is the maximum computed shear stress change and ρ_{min} depends on the assumed initial conditions. For $\Delta\tau$ assigned, as in the present study, and experimental values of a this implies the existence of a maximum value $\sigma_0^{max}=\Delta\tau/(a\rho_{min})$ to have instantaneous triggering.

To explain instantaneous triggering of the 26 s and 30 s events, the σ_0 values reported in Table 3 could be increased up to σ_0^{max}~hundreds of bars for close to failure initial conditions (V_i>cm/yr and $T(t=0)>L/V_i$) or if the perturbing stress was applied close to the unperturbed failure time. This estimate of σ_0^{max} is compatible with high pore pressure values at seismogenic depth, possibly related to the vicinity of 26 s and 30 s events to the WVZ and the Reykjanes ridge. In fact greater than hydrostatic pore pressure values are expected and observed in hot regions, such as the ductile roots of faults (Rice, 1992), where rocks may behave as plastic with low permeabilities values.

4. Conclusive remarks

We had the rare opportunity to consider evidences of early aftershocks both in near field and in far field conditions. We analyzed three of the major early aftershocks occurring in the first minutes after the mainshock in the South Iceland Seismic Zone in terms of dynamic stress interaction or triggering. With a one-dimensional model of a perturbed fault, the two aftershocks occurring in the Reykjanes Peninsula can be reproduced as triggered dynamically, that is for these events we estimated a failure time that correlates with the measured origin time. Unlike other fault rheology laws, the rate- and state-dependent fault rheology requires low values of effective normal prestress to allow instantaneous triggering effects.

5. References

Arnadottir, T., S. Jonsson, R. Pedersen, and G. B. Gudmundsson (2003), Coulomb stress changes in the South Iceland Seismic Zone due to two large earthquakes in June 2000, Geophys. Res. Lett., 30 (5), doi:10.1029/2002GL016495.

Cotton, F., and O. Coutant (1997), Dynamic stress variations due to shear faults in a plane layered medium, Geophys. J. Int., 128, 676-688.

Linker, M. F., and J H. Dieterich (1992), Effects of variable normal stress on rock friction: observations and constitutive equations, J Geophys. Res., 97(4), 4932-4940.

Pedersen, R., S. Jonsson, T. Arnadottir, F. Sigmundsson, and K.L. Feigl (2003), Fault slip distribution of two June 2000 M_W 6.5 earthquakes in South Iceland estimated from joint inversion of InSAR and GPS measurements, Earth Planet. Sci Lett, 213(3-4), 487-502.

Rice, J. (1992), Fault stress states, pore pressure distributions, and the weakness of the San Andreas fault. Fault mechanics and transport properties of rocks. A Festschrift in Honor of W. F. Brace (based on June 1990 symposium at MIT). edited by Brian Evans and Teng-Fong Wong, Academic Press, London, 475-503.